CCT-K6.2 NIST – NMIJ/AIST
Final Report 05-03-2020, approved by NIST and NMIJ

BILATERAL KEY COMPARISON CCT-K6.2 ON HUMIDITY STANDARDS IN THE FROST-POINT TEMPERATURE RANGE FROM –80 °C TO -30 °C

C.W. Meyer[1] and H. Abe[2]

[1]National Institute of Standards and Technology (NIST), USA
[2] National Metrology Institute of Japan (NMIJ), Japan

Abstract

A Consultative Committee on Thermometry (CCT) Key Comparison of frost point temperatures was carried out by the National Institute of Standards and Technology (NIST, USA) and the National Metrology Institute of Japan (NMIJ, Japan) between December 2015 and November, 2016. The results of this comparison are reported here, along with descriptions of the humidity laboratory standards for NIST and NMIJ/AIST and the uncertainty budget for these standards. This report also describes the protocol for the comparison and presents the data acquired. The results are analyzed, determining degree of equivalence between the frost-point standards of NIST and NMIJ.

Keywords: Comparison, Humidity, Frost Point, Degree of Equivalence.

1. Introduction

Key Comparisons determine differences between measurement standards of different National Metrology Institutes (NMIs). They play an important role in ensuring that the standards of all NMIs are in agreement.

At its 20th meeting in April 2000, the Consultative Committee for Thermometry (CCT) called for a Key Comparison on humidity standards to be conducted by all major National Metrology Institutes. It asked CCT Working Group 6, WG6, (now CCT Working Group on Humidity Measurements, WG-Hu) to draw up a technical protocol for a CIPM key comparison named "CCT-K6". The National Physical Laboratory (UK) and the National Metrology Institute of Japan were chosen to be the pilot laboratory and assistant pilot laboratory, respectively. The National Institute of Standards and Technology (NIST, USA) participated in this key comparison. In 2015 the comparison report [1] was published.

For its participation in CCT-K6, NIST used two humidity generators. For the frost points of –50 °C and –30 °C, the NIST Low Frost-point Generator (LFPG) was used, and for the dew/frost points at –10 °C, 1 °C, and 20 °C the NIST Hybrid Humidity Generator (HHG) was used. However, maintenance of the NIST LFPG had always been cumbersome, and it was frequently out of operation and in need of repair. Since 2013 NIST has used the HHG instead of the LFPG to provide NIST humidity standards over the range –85 °C to 0 °C. In 2016 NIST decided to end support of the LFPG.

Because the NIST LFPG was no longer used for providing NIST humidity standards, it was necessary for NIST to provide linkage of the HHG frost-points below –10 °C to the CCT-K6 Key Comparison Reference Values (KCRV). NIST invited NMIJ to participate in a bilateral comparison of frost-points at the points –50 °C and –30 °C. NMIJ/AIST agreed to perform the comparison, and in addition NIST and NMIJ agreed to perform frost-point comparisons at two points not covered in CCT-K6: –80 °C and –70 °C. The comparison was carried out between December 2015 and November 2016, and it was designated CCT-K6.2. NIST was the pilot for this bilateral comparison. This bilateral comparison followed the same technical procedures for each frost point as for the CCT-K6, except that only one transfer standard was used.

2. Participants

NIST	**Christopher Meyer** National Institute of Standards and Technology 100 Bureau Drive Gaithersburg, MD 20899 USA	Tel.: +1-301-975-4825 Fax: +1-301-548-0206 e-mail : cmeyer@nist.gov
NMIJ	**Hisashi Abe** NMIJ AIST Tsukuba Central 3-1 Tsukuba 305-8563 Japan	Tel.: +81-29-861-6845 Fax: +81-29-861-6854 e-mail : abe.h@aist.go.jp

3. Comparison Method

The comparison between frost-point temperatures realized at NIST and NMIJ was performed through use of a transfer standard (a chilled-mirror hygrometer). At a given nominal frost point, each participant used its generator to produce moist air having a frost-point temperature determined to be $T_{\mathrm{FP}}^{\mathrm{g}}$. The transfer standard then measured the dew/frost-point temperature of the generated gas, $T_{\mathrm{FP}}^{\mathrm{m}}$. The difference between the two values was

$$\Delta T_{\mathrm{FP}} = T_{\mathrm{FP}}^{\mathrm{g}} - T_{\mathrm{FP}}^{\mathrm{m}} .$$

The comparison of NIST and NMIJ humidity standards was then performed by comparing the values of ΔT_{FP} determined using the NIST humidity generator, $\Delta T_{\mathrm{FP}}(\mathrm{NIST})$, with those of the NMIJ humidity generator, $\Delta T_{\mathrm{FP}}(\mathrm{NMIJ})$.

4. Generators

The NIST humidity generator used was the NIST Hybrid Humidity Generator (HHG). Its principle of operation depends on the desired value of $T_{\mathrm{DP/FP}}$.

For $T_{DP/FP} \geq -15$ °C, the HHG operates as a conventional two-pressure generator, saturating air with water at a temperature T_s and pressure P_s to produce moist air with a molar fraction x_g given by

$$x_g = \frac{e(T_s)}{P_s} \; f(T_s, P_s). \qquad 1)$$

Here, $e(T_s)$ is the water vapor pressure at T_s, calculated using [2-3] and $f(T_s, P_s)$ is the water-vapor enhancement factor, calculated using [4]. The saturator temperature is measured by a standard platinum resistance thermometer (SPRT) immersed in the same temperature-controlled bath as the saturator. The saturator pressure, which can vary from ambient to 500 kPa, is measured by a strain-gauge pressure transducer that is connected by a tube to the saturator at a point near its outlet.

For $T_{DP/FP} \leq -15$ °C, the HHG uses the divided flow method, which involves diluting the saturated gas with dry gas using precisely-metered streams of gas. The molar fraction after dilution is

$$x_g = \frac{\dot{n}_s x_s + \dot{n}_p x_p}{\dot{N}}, \qquad 2)$$

where $\dot{n}_s$ and $\dot{n}_p$ are the molar flows of the saturated gas and pure (dry) gas, respectively, and $\dot{N}$ is the total molar flow. Also, x_s is the molar fraction of water in the saturated gas and x_p is the residual molar fraction of water in the pure gas. For the HHG in divided flow mode, the saturator is operated at a temperature of 1 °C and a pressure of 300 kPa, resulting in $x_s \approx 0.0022$.

The generated frost-point temperature is obtained from x_g by measuring the pressure P_c using a strain-gauge pressure transducer at the inlet of the chilled-mirror hygrometer. T_{FP} is then obtained by iteratively solving the equation

$$x_g = \frac{e_i(T_{FP})}{P_c} \; f(T_{FP}, P_c), \qquad 3)$$

where e_i is the saturated vapor pressure for ice, calculated using [5-6]. The value of $f(T_{FP}, P_s)$ is calculated using [4]. A more complete description of the NIST HHG may be found in [7].

To ensure the stability of the HHG results, the HHG pressure gauges are calibrated yearly. The HHG SPRT resistance at the triple point of water R_{TPW} is also calibrated yearly. The pressure gauge and SPRT calibrations are performed at NIST. The policy of the HHG laboratory is that if the change in R_{TPW} from that of the original calibration ever corresponds to a temperature drift of more than 10 mK, a full calibration will be performed. Finally, NIST employs check standards during every customer calibration for the purpose of detecting any possible errors or long-term drifts.

The NMIJ humidity generators used were the Frost-Point Generator (FPG) [8] and the Magnetic Suspension Balance/Diffusion-Tube humidity Generator (MSB/DTG) [9] for the nominal T_{FP} of –30 °C to –70 °C and at –80 °C, respectively.

The FPG is a single-pressure generator, consisting of a temperature-controlled bath and a saturator with a heat exchanger. The heat exchanger is a stainless-steel tube coil and the saturator is a stainless-steel box. The stainless-steel box has the inlet hole and outlet hole, where the heat exchanger and the outlet tube, respectively, are welded. The heat exchanger and the saturator are immersed in the temperature-controlled bath filled with ethanol. The dry N_2 introduced into the inlet of the FPG first passes through the heat exchanger and then the saturator. The inside of the saturator is a horizontal zigzag tunnel with a height of 20 mm. The half of the tunnel (10 mm) is filled with ice of deionized water. The total length of the tunnel is approximately 2 m. The saturator temperature T_s and saturator pressure P_s are measured using a standard platinum resistance thermometer and a strain-gauge pressure transducer, respectively. The chilled mirror hygrometer is connected to the outlet of the FPG. The pressure at the outlet P_o is also measured using another strain-gauge pressure transducer. T_{FP} of the N_2 humidified by the FPG can be calculated using the following equation:

$$\frac{e_i(T_{FP})f(P_o,T_{FP})}{P_o} = \frac{e_i(T_s)f(P_s,T_s)}{P_s}, \qquad 4)$$

where $e_i(T)$ is the saturation water vapor pressure of ice [10] at temperature T, and $f(P, T)$ is the enhancement factor [11] at pressure P and temperature T. Note that $P_s \approx P_o$ in eq. 4) because the FPG is a single pressure generator.

The MSB/DTG is a trace-moisture generator based on the diffusion tube method. The generation chamber of the DTG is attached to the bottom of the MSB with a common vacuum flange to form a closed system with the MSB. The MSB consists of magnetic suspension coupling and an analytical balance. A diffusion cell (a small water container with a diffusion tube) in the generation chamber is magnetically suspended from the measuring load of the magnetic suspension coupling without contact with the analytical balance using the permanent magnet and the electromagnet. The pressure inside the chamber is controlled to 155 kPa using a pressure regulator. The temperature of the chamber is maintained at 25 °C or 60 °C. The water vapor from the diffusion cell is mixed with the dry N_2 introduced from the inlet of the generation chamber. This humid gas is taken out from the outlet of the generation chamber and further mixed with the dry N_2 flowing from the bypass line. The evaporation rate of water vapor from the diffusion cell N is measured as the mass-loss rate of the diffusion cell using the MSB. The total flow rate of the dry nitrogen F is accurately and precisely measured and controlled using a flow measurement/control system [12] which uses a mass flow meter composed of multiple critical flow Venturi nozzles (CFVNs), also known as sonic nozzles. The molar fraction of water vapor in nitrogen gas x_w is calculated by

$$x_w = \frac{N + N_b + F x_b/(1 - x_b)}{N + N_b + F + F x_b/(1 - x_b)}, \quad 5)$$

where N_b is the amount-of substance of water vapor desorbed per unit time from the inside surfaces of the generation chamber and tubes used for the pipewok, and x_b is the molar fraction of residual water in dry N_2. Using eqs. 4) and 5), T_{FP} of the N_2 humidified by the MSB/DTG is given by

$$\frac{e_1(T_{FP})\, f(P_o, T_{FP})}{P_o} = x_w . \quad 6)$$

5. Transfer standard

Instrument type:	Chilled-mirror hygrometer
Measurand	dew/frost-point temperature
Model:	RH Systems 373LX*
Serial Number:	15-0103
Size (in Packing case):	63 cm x 53 cm x 40 cm
Weight (in Packing case):	31.2 kg
Manufacturer:	RH Systems, USA
Owner:	RH Systems, USA
Electrical supply:	220 V / 50 Hz
Approximate value for insurance and customs declaration:	US$ 88,250.00

6. Measurement process

Sample air with $T_{DP/FP}$ realized by a participant's standard generator was introduced into the inlet of a transfer-standard hygrometer through a stainless-steel tube. The tube was attached to the transfer standard using a ¼" VCR fitting. A 100-ohm platinum resistance thermometer (PRT) embedded beneath the surface of the transfer standard's mirror measured the frost-point temperature. The current applied through the PRT was nominally 1 mA. At NIST, the resistance of the PRT was measured using a commercial AC resistance bridge using a 100 Ω standard resistor as its reference. At NMIJ, the resistance of the PRT was measured using a digital multimeter calibrated using an AC resistance bridge with a 100 Ω standard resistor as its reference. For both NIST and NMIJ, the measured resistance was converted to a nominal frost-point temperature using the reference function given in IEC 60751, as described in Appendix 3 of the CCT-K6 protocol.

* The commercial product mentioned here is included for completeness only and does not constitute an endorsement by NIST nor does it imply that this product is necessarily the best available for its purpose.

A total of four dew/frost-point temperatures were used for the comparison: –80 °C, –70 °C, –50 °C, and –30 °C. Each participant made four independent measurements for each frost-point temperature, reforming the condensate on the hygrometer's mirror each time. At each measured frost point, the PRT resistance readings were monitored until they reached the laboratory's criterion for being in a steady state. At NIST, typical monitoring periods at –80 °C, –70 °C, –50 °C, and –30 °C were 48 h, 48 hr, 3 h, and 1 h, respectively. At NMIJ, the monitoring periods at –80 °C (MSB/DTG) and –70 °C to –30 °C (FPG) were 6 h and 5.5 h, respectively. Afterwards, multiple readings of the resistance of the PRT were recorded, and the mean and standard deviation of these readings were recorded.

7. Measurement data

Table 1 shows the results of the generator/hygrometer comparisons for both NIST and NMIJ. Table 2 shows the difference between generated and measured frost-point temperatures ΔT_{FP} for four measurements. For a given nominal value of ΔT_{FP}, the results of NIST and NMIJ are shown on separate rows. The results for each of the four measurements are shown in separate columns. The mean and standard deviation of these measurements are shown in the last two columns. The data shown in Table 2 is plotted in Fig. 1. We note that there is unusually large scatter in the NIST results at –50 °C and in the NMIJ results at –70 °C. We are not sure why there was such large scatter at these points, but we believe they were due to problems with stability of the transfer standard; our check standards did not exhibit such large variations at these points.

8. Comparison Uncertainty

For a set of determinations of ΔT_{FP} made at a nominal T_{FP} the standard uncertainty of the generator/hygrometer comparison $u_c(\Delta T_{FP})$ is given by

$$u_c(\Delta T_{FP}) = \left[u_A^2(\Delta T_{FP}) + u^2\left(T_{FP}^g\right) + u^2\left(T_{FP}^m\right)\right]^{1/2} . \qquad 7)$$

Descriptions of $u_A(\Delta T_{FP})$, $u\left(T_{FP}^g\right)$, and $u\left(T_{FP}^m\right)$ are given below. First, $u_A(\Delta T_{FP})$ is the type A uncertainty for the determination of ΔT_{FP}. This uncertainty includes the reproducibility of the generator, the chilled-mirror hygrometer, and the multimeter making the resistance measurements. Secondly, $u\left(T_{FP}^g\right)$ is the type B uncertainty of the generated value of T_{FP}. The source of the values $u\left(T_{FP}^g\right)$ for NIST is [7], which contains a complete uncertainty budget for the NIST Hybrid Humidity Generator. The source of the values $u\left(T_{FP}^g\right)$ for NMIJ is [8, 9], which provides an uncertainty analysis for the FPG and MSB/DTG. Table 3 shows the major uncertainty elements and their standard uncertainty values for the NIST generator, for the four nominal values of T_{FP}. Table 4 shows the contribution of these uncertainty elements to $u\left(T_{FP}^g\right)$. Similarly, Tables 5 shows the values of these standard uncertainties for the NMIJ generator and Table 6 shows their contribution to $u\left(T_{FP}^g\right)$ for NMIJ. Note that the NMIJ uncertainties provided for the water vapor pressure and enhancement factor for the FPG are zero because the generator is single pressure.

Table 1. Results of generator/hygrometer comparisons.

Hygrometer RH Systems 373LX, S/N 15-0103					
Nominal T_{FP} (°C)	Meas. #	Realized T_{FP} (°C)	Measured PRT Resistance (Ω)	Measured T_{FP} (°C)	ΔT_{FP} (°C)
NIST					
–30	1	-30.075	88.1551	-30.169	0.093
–30	2	-30.046	88.1660	-30.141	0.096
–30	3	-30.042	88.1697	-30.132	0.090
–30	4	-30.060	88.1604	-30.155	0.095
NMIJ					
–30	1	-29.987	88.1898	-30.081	0.094
–30	2	-29.987	88.1903	-30.080	0.092
–30	3	-29.988	88.1908	-30.078	0.090
–30	4	-29.987	88.1907	-30.078	0.091
NIST					
–50	1	-49.932	80.2681	-50.096	0.164
–50	2	-49.998	80.2678	-50.097	0.099
–50	3	-50.002	80.2755	-50.077	0.076
–50	4	-50.010	80.2722	-50.086	0.076
NMIJ					
–50	1	-49.993	80.2706	-50.090	0.097
–50	2	-49.994	80.2720	-50.086	0.093
–50	3	-49.994	80.2728	-50.084	0.091
–50	4	-49.994	80.2732	-50.083	0.090
NIST					
–70	1	-69.962	72.3374	-69.993	0.031
–70	2	-70.071	72.2861	-70.121	0.050
–70	3	-70.042	72.2941	-70.101	0.059
–70	4	-70.055	72.2944	-70.100	0.045
NMIJ					
–70	1	-69.996	72.2892	-70.113	0.117
–70	2	-69.995	72.2881	-70.116	0.121
–70	3	-69.995	72.3125	-70.055	0.060
–70	4	-69.997	72.3102	-70.061	0.064
NIST					
–80	1	-80.105	68.3057	-80.049	-0.056
–80	2	-80.195	68.2477	-80.194	-0.001
–80	3	-80.219	68.2406	-80.211	-0.008
–80	4	-80.140	68.2624	-80.157	0.017
NMIJ					
–80	1	-80.117	68.3173	-80.020	-0.097
–80	2	-80.106	68.3090	-80.041	-0.064
–80	3	-80.097	68.3055	-80.050	-0.047
–80	4	-80.125	68.3050	-80.051	-0.074

Table 2. Difference between realized and measured dew/frost-point temperatures $\Delta T_{DP/FP}$ for NIST and NMIJ

Nominal T_{FP} (°C)	NMI	Meas. 1 ΔT_{FP} (°C)	Meas. 2 ΔT_{FP} (°C)	Meas. 3 ΔT_{FP} (°C)	Meas. 4 ΔT_{FP} (°C)	$\overline{\Delta T_{FP}}$ (°C)	$\sigma(\Delta T_{FP})$ (°C)
−30	NIST	0.093	0.096	0.090	0.095	0.094	0.003
−30	NMIJ	0.094	0.092	0.090	0.091	0.092	0.002
−50	NIST	0.164	0.099	0.076	0.076	0.104	0.042
−50	NMIJ	0.097	0.093	0.091	0.090	0.093	0.003
−70	NIST	0.031	0.050	0.059	0.045	0.046	0.012
−70	NMIJ	0.117	0.121	0.060	0.064	0.091	0.033
−80	NIST	-0.056	-0.001	-0.008	0.017	-0.012	0.031
−80	NMIJ	-0.097	-0.064	-0.047	-0.074	-0.071	0.021

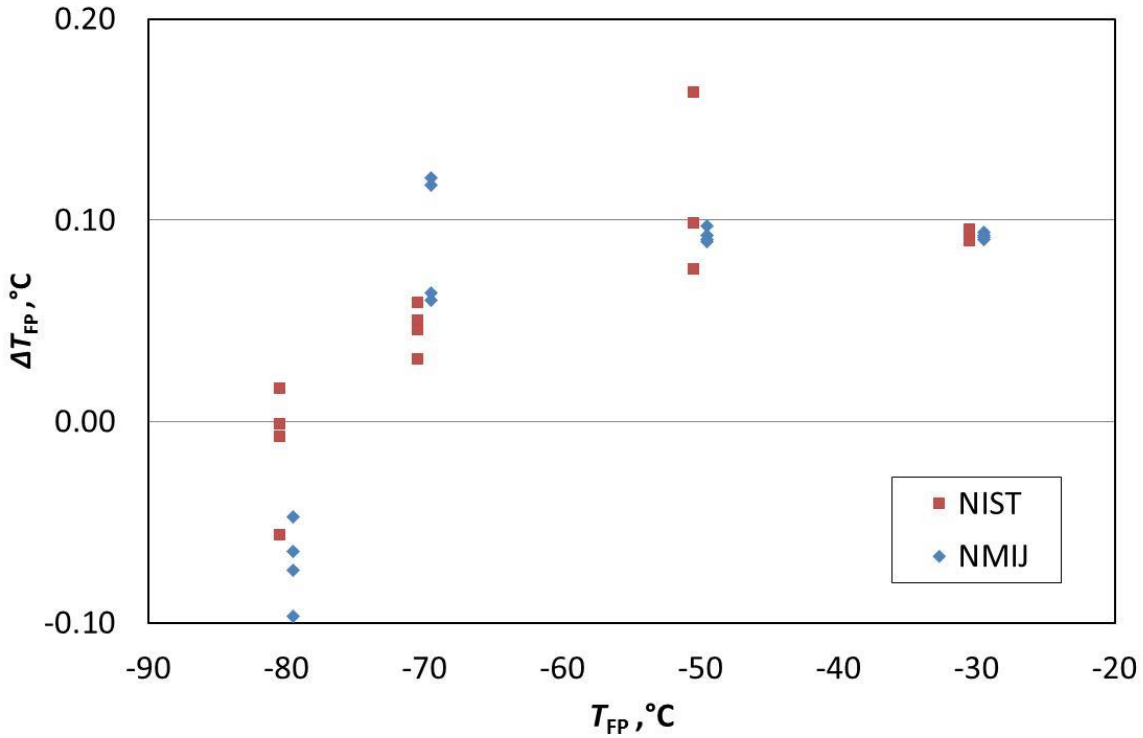

Figure 1. Difference between realized and measured dew/frost-point temperatures $\Delta T_{DP/FP}$ for NIST and NMIJ. Note: data from the two NMIs are slightly offset horizontally to facilitate viewing.

Table 3. Uncertainty elements and their standard uncertainty values for the NIST generator, for the four nominal values of T_{FP}.

Uncertainty for NIST generator at T_{FP} =	**-30 °C**	**-50 °C**	**-70 °C**	**-80 °C**
Saturator Temperature Measurement				
Calibration uncertainty	0.001 °C	0.001 °C	0.001 °C	0.001 °C
Long-term stability	0.001 °C	0.001 °C	0.001 °C	0.001 °C
Saturator Pressure Measurement				
Calibration uncertainty	42 Pa	42 Pa	42Pa	42 Pa
Long-term stability	7 Pa	7 Pa	7 Pa	7 Pa
Hygrometer Pressure Measurement				
Calibration uncertainty	18 Pa	18 Pa	18 Pa	18 Pa
Long-term stability	7 Pa	7 Pa	7 Pa	7 Pa
Flow measurement				
Calibration uncertainty	0.05%	0.05%	0.05%	0.05%
Long-term stability	0.02%	0.02%	0.02%	0.02%
Moisture in dry gas	1 nmol/mol	1 nmol/mol	1 nmol/mol	1 nmol/mol
Water Adsorption/desorption on tube walls	1 nmol/mol	1 nmol/mol	1 nmol/mol	1 nmol/mol
Calculation:				
Saturation vapor pressure formula(e)	0.03 Pa	0.02 Pa	0.02 Pa	0.02 Pa
Water vapor enhancement formula(e)	0.0006	0.0006	0.0007	0.0008

Table 4. Contribution of the uncertainty elements in Table 3 to $u\left(T_{FP}^{g}\right)$ for NIST, in °C, for the four nominal values of T_{FP}. The combined standard uncertainty is shown in the last row.

Uncertainty for NIST generator at T_{FP} =	**-30 °C**	**-50 °C**	**-70 °C**	**-80 °C**
Saturator Temperature Measurement				
Calibration uncertainty	0.001	0.001	0.0005	0.0004
Long-term stability	0.001	0.001	0.0005	0.0004
Saturator Pressure Measurement				
Calibration uncertainty	0.001	0.001	0.001	0.001
Long-term stability	0.0002	0.0002	0.0001	0.0001
Hygrometer Pressure Measurement				
Calibration uncertainty	0.001	0.001	0.001	0.001
Long-term stability	0.0006	0.0005	0.0004	0.0004
Flow measurement:				
Calibration uncertainty	0.005	0.005	0.004	0.004
Long-term stability	0.002	0.002	0.002	0.001
Moisture in dry gas	0.00003	0.0002	0.003	0.012
Water Adsorption/desorption on tube walls	0.00003	0.0002	0.003	0.012
Calculation:				
Saturation vapor pressure formula(e)	0.006	0.009	0.011	0.013
Water vapor enhancement formula(e)	0.006	0.006	0.005	0.005
Combined standard uncertainty:	**0.010**	**0.012**	**0.014**	**0.022**

Table 5. Uncertainty elements and their standard uncertainty values for the NMIJ generator. For the highest three nominal values of T_{FP}, the FPG was used and at -80 °C the MSB/DTG was used.

Uncertainty for NMIJ generator at T_{FP} =	**-30 °C**	**-50 °C**	**-70 °C**	**-80 °C**
Saturator Temperature Measurement				
Sensor uncertainty	0.009 °C	0.009 °C	0.009 °C	-----
Temperature Homogeneity	0.006 °C	0.006 °C	0.006 °C	-----
Temperature Stability	0.004 °C	0.004 °C	0.004 °C	-----
Saturator Pressure Measurement				
Calibration uncertainty	1.4 Pa	1.4 Pa	1.4 Pa	-----
Long-term stability	21.1 Pa	21.1 Pa	21.1 Pa	-----
Effect of Tubing	78.8 Pa	78.8 Pa	78.8 Pa	-----
Hygrometer Pressure Measurement				
Calibration uncertainty	1.4 Pa	1.4 Pa	1.4 Pa	5 Pa
Pressure stability	21.1 Pa	21.1 Pa	21.1 Pa	10 Pa
Effect of Tubing	8.5 Pa	8.5 Pa	8.5 Pa	20 Pa
Saturator Efficiency	0.016 °C	0.014 °C	0.012 °C	-----
Water Adsorption/desorption on tube walls	0.0002	0.0019	0.0341	0.0002
Trace moisture generation by MSB/DTG	-----	-----	-----	2.36 nmol/mol
Calculation:				
Saturation vapor pressure formula(e)	0 Pa	0 Pa	0 Pa	0.5 %
Water vapor enhancement formula(e)	0	0	0	0.2 %

Table 6. Contribution of the uncertainty elements in Table 5 to $u\left(T_{\mathrm{FP}}^{\mathrm{g}}\right)$ for NMIJ, in °C. For the highest three nominal values of T_{FP}, the FPG was used and at -80 °C the MSB/DTG was used.

Uncertainty for NMIJ generator at T_{FP} =	**-30 °C**	**-50 °C**	**-70 °C**	**-80 °C**
Saturator Temperature Measurement				
Sensor uncertainty	0.009	0.009	0.009	-----
Temperature Homogeneity	0.006	0.006	0.006	-----
Temperature Stability	0.004	0.004	0.004	-----
Saturator Pressure Measurement				
Calibration uncertainty	0.0001	0.0001	0.0001	-----
Long-term stability	0.002	0.002	0.001	-----
Effect of Tubing	0.007	0.006	0.005	-----
Hygrometer Pressure Measurement				
Calibration uncertainty	0.0001	0.0001	0.0001	0.0001
Long-term stability	0.002	0.002	0.001	0.001
Effect of Tubing	0.001	0.001	0.001	0.001
Saturator Efficiency	0.016	0.014	0.012	-----
Water Adsorption/desorption on tube walls	0.002	0.015	0.229	0.0013
Trace moisture generation by MSB/DTG	-----	-----	-----	0.013
Calculation:				
Saturation vapor pressure formula(e)	0.000	0.000	0.000	0.030
Water vapor enhancement formula(e)	0.000	0.000	0.000	0.012
Combined standard uncertainty:	**0.021**	**0.025**	**0.230**	**0.035**

Finally, $u\left(T_{\mathrm{FP}}^{\mathrm{m}}\right)$ is the type B uncertainty of the measured value of T_{FP}. It is given by the type B uncertainty of the resistance measurement system measuring the resistance of the PRT in the chilled mirror hygrometer. The values of $u\left(T_{\mathrm{FP}}^{\mathrm{m}}\right)$ were 0.001 °C for NIST and 0.001 °C for NMIJ.

Table 7 shows the calculated value of $u_{\mathrm{c}}(\Delta T_{\mathrm{FP}})$ and its components for each value of T_{FP} and each participating NMI.

Table 7. Standard uncertainty of the determinations of ΔT_{FP} for NIST and NMIJ. The column headings are described in the text.

Nominal $T_{DP/FP}$ (°C)	Participating Institute	$u_A(\Delta T_{FP})$ (°C)	$u(T_{FP}^{g})$ (°C)	$u(T_{DP/FP}^{m})$ (°C)	$u_c(\Delta T_{DP/FP})$ (°C)
−30	NIST	0.003	0.010	0.001	0.010
−30	NMIJ	0.002	0.021	0.001	0.021
−50	NIST	0.042	0.012	0.001	0.044
−50	NMIJ	0.003	0.025	0.001	0.025
−70	NIST	0.012	0.014	0.001	0.018
−70	NMIJ	0.033	0.23	0.001	0.232
−80	NIST	0.031	0.022	0.001	0.038
−80	NMIJ	0.021	0.035	0.001	0.041

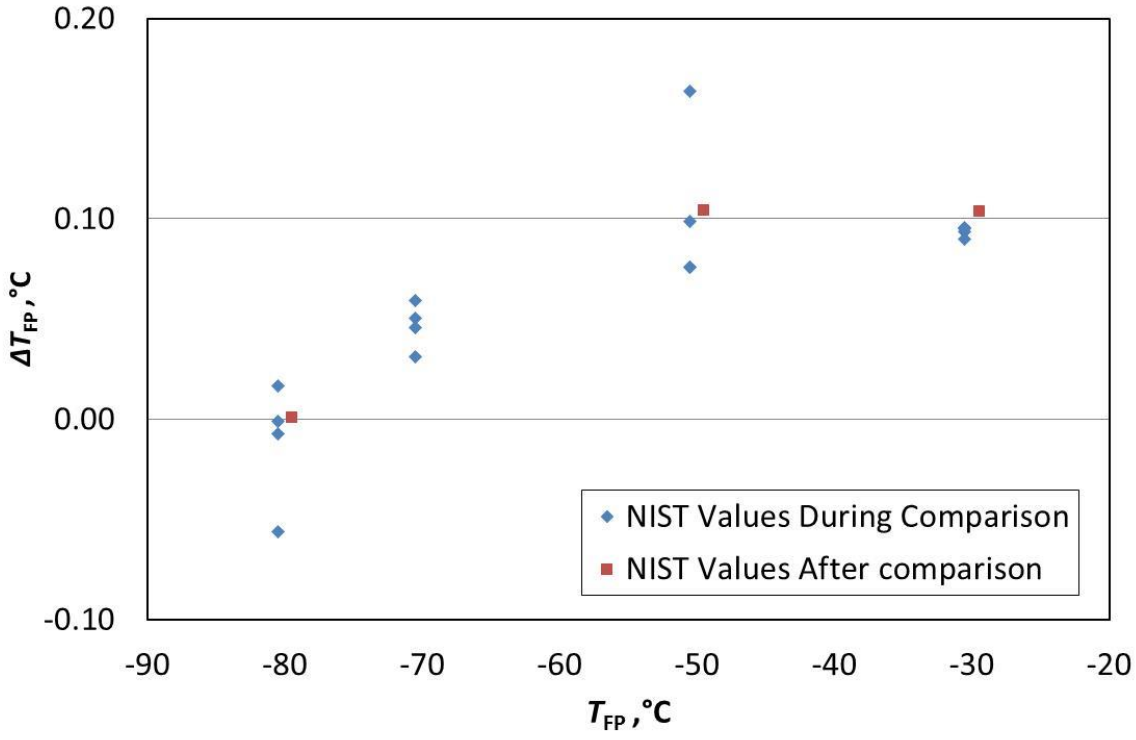

Figure 2. Difference between the NIST generator/hygrometer comparisons performed in December 2015-February 2016 and in November 2016.

9. Drift of Transfer Standard

The first generator/hygrometer comparison measurements were made at NIST in December 2015-February 2016. Afterwards, the transfer standard was sent to NMIJ so that it could perform its comparison measurements. The transfer standard was returned to NIST in October 2016, and the next comparison measurements were made in November 2016.

Drift of the transfer standard during the course of the NIST-NMIJ comparison may be estimated by examining the difference between the NIST generator/hygrometer comparisons performed in December 2015-February 2016 and November 2016. This difference is shown in Fig. 2. The average magnitude of the difference between the December 2015-February 2016 comparisons and the November 2016 comparisons is approximately 0.008 °C. In our uncertainty budget we have added a type B uncertainty component due to the possibility of transfer standard drift. Based on the results of Fig. 2, we have estimated it to contribute a standard uncertainty of 0.005 °C $(0.008\ ^\circ\mathrm{C}/\sqrt{3})$ to the NIST-NMIJ/AIST comparison.

10. Degree of Equivalence

We define the degree of equivalence between the values of T_{FP} realized by NMIJ and those of NIST, $D_{NIST/NMIJ}$ as

$$D_{NIST/NMIJ}\ (T_{FP}) \equiv [\Delta T_{FP}]_{NIST} - [\Delta T_{FP}]_{NMIJ}\ . \qquad 8)$$

The uncertainty of the degree of equivalence $u(D_{NIST/NMIJ}\ (T_{FP})$ is the combination of $u_c(\Delta T_{FP})$ for NIST, $u_c(\Delta T_{FP})$ for NMIJ, and the uncertainty u_{drift} due to possible drift of the transfer standard:

$$u[D_{NIST/NMIJ}\ (T_{FP})] = \left\{ [u_c^2(\Delta T_{FP})]_{NIST} + [u_c^2(\Delta T_{FP})]_{NMIJ} + u_{drift}^2 \right\}^{1/2}. \qquad 9)$$

The expanded (k=2, 95% confidence level) uncertainty for the degree of equivalence is

$$U(D_{NIST/NMIJ}) = 2u(D_{NIST/NMIJ}), \qquad 10)$$

The results are presented in Table 8 and plotted in Fig. 3. All values of $D_{NIST\text{-}NMIJ/AIST}$ are within the expanded uncertainties.

Table 8. Degree of equivalence between T_{FP} realized by NMIJ/AIST and that of NIST, and its expanded uncertainty (k = 2) in a comparison of four frost points.

Nominal $T_{DP/FP}$ (°C)	$D_{NIST/NMIJ}$ (°C)	$U(D_{NIST/NMIJ})$ (°C)
−30	0.002	0.048
−50	0.011	0.101
−70	−0.045	0.466
−80	0.059	0.112

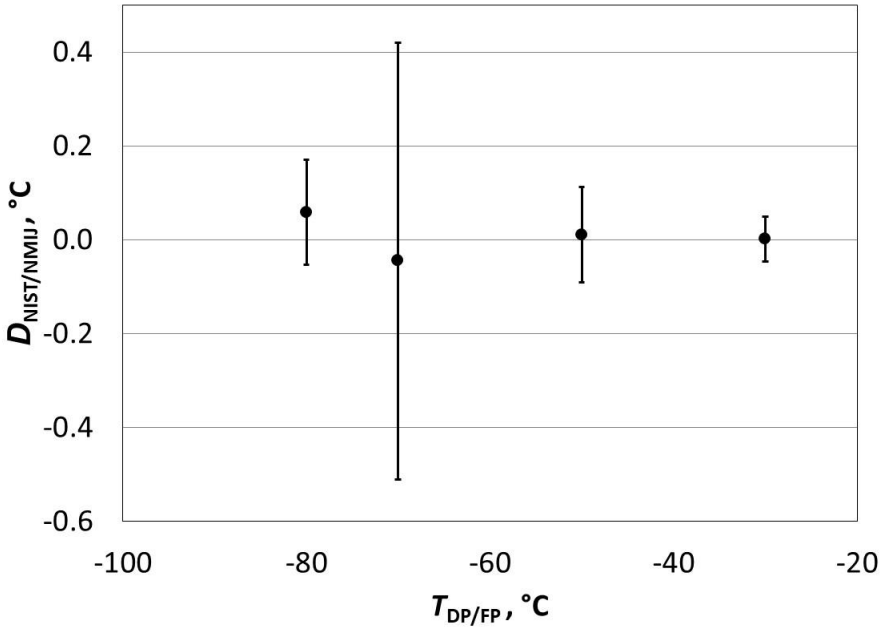

Figure 3. The degree of equivalence $D_{NIST\text{-}NMIJ/AIST}$ between the four frost-point temperatures realized by the standard generators of NIST, $[T_{FP}]_{NIST}$, and that of NMIJ, $[T_{FP}]_{NMIJ}$ as defined in Eq. 8. The uncertainty bars represent the expanded (k = 2) uncertainty of the degree of equivalence, as defined in Eq. 10.

11. Linkage to the CCT-K6 KCRV

Both NIST and NMIJ participated in the CCT-K6 multilateral key comparison. However, the generator that NIST is now using is different from that used in the comparison at the -30 °C and -50 °C points, while the generator that NMIJ is using is the same. Therefore, the current NIST realization of those frost points using the HHG may be linked to the key comparison reference values (KCRV) for T_{FP} [1] through this bilateral comparison. The

degree of equivalence between T_{FP} realized by a NMI and the KCRV, $D_{NMI/KCRV}$, is defined as

$$D_{NMI/KCRV}\ (T_{FP}) \equiv [\Delta T_{FP}]_{NMI} - [\Delta T_{FP}]_{KCRV}\ . \qquad 11)$$

Eq. 8 and Eq. 11 may be used to determine $D_{NIST/KCRV}$:

$$D_{NIST/KCRV}\ (T_{FP}) = D_{NIST/NMIJ}\ (T_{FP}) + D_{NMIJ/KCRV}\ (T_{FP})\,. \qquad 12)$$

with corresponding uncertainty

$$U^2(D_{NIST/KCRV}) = U^2(D_{NIST/NMIJ}) + U^2(D_{NMIJ/KCRV})\,. \qquad 13)$$

The relevant values of $D_{NMIJ/KCRV}$ and $U(D_{NMIJ/KCRV})$ from [1] are given in Table 9:

Table 9. Degree of equivalence between $T_{DP/FP}$ realized by NMIJ and the KCRV, $D_{NMIJ/KCRV}$, and its expanded uncertainty (k = 2), $U(D_{NMIJ/KCRV})$, at T_{FP} values of −30 °C and −50 °C, as given by Tables 7.3 and 7.4 in [1].

Nominal T_{FP} (°C)	$D_{NMIJ/KCRV}$ (°C)	$U(D_{NMIJ/KCRV})$ (°C)
−30	-0.050	0.057
−50	-0.023	0.100

Combining the results of Tables 8-9 using Eqs. 12-13 yields the values of $D_{NIST/KCRV}$ and $U(D_{NIST/KCRV})$:

Table 10. Degree of equivalence between T_{FP} realized by NIST and the KCRV, $D_{NIST/KCRV}$, and its expanded uncertainty (k = 2), $U(D_{NIST/KCRV})$, at T_{FP} values of −30 °C and −50 °C.

Nominal $T_{DP/FP}$ (°C)	$D_{NIST/KCRV}$ (°C)	$U(D_{NIST/KCRV})$ (°C)
−30	−0.048	0.075
−50	−0.012	0.142

The values of $D_{NIST/KCRV}$ are all within the k=2 uncertainty values $U(D_{NIST/KCRV})$.

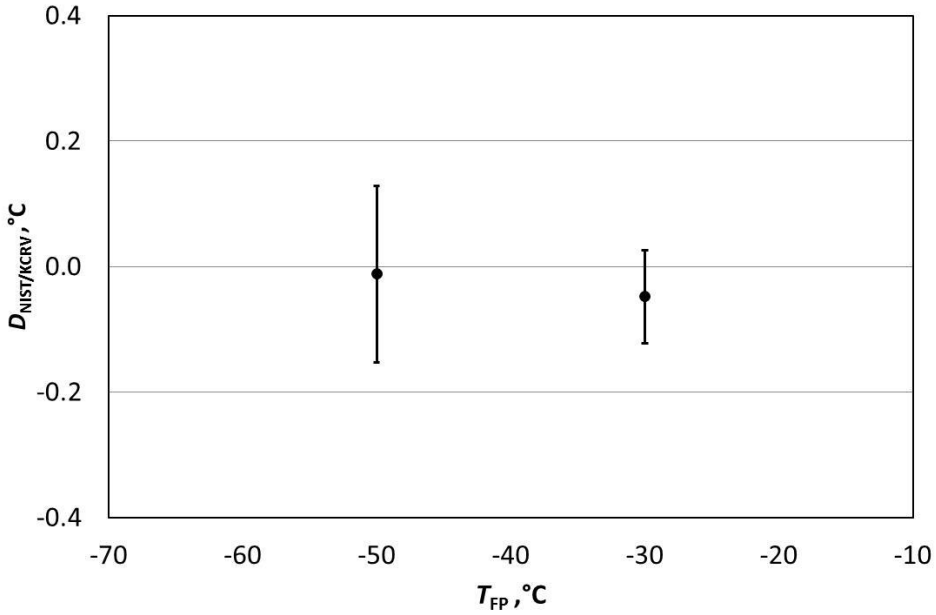

Figure 4. The degree of equivalence $D_{NIST/KCRV}$ between the dew/frost-point temperatures realized by the standard generator of NIST, $[T_{FP}]_{NIST}$ and the key comparison reference values (KCRVs), $[T_{FP}]_{KCRV}$, as determined by Eq. 9. The uncertainty bars represent the expanded (k = 2) uncertainty of the degree of equivalence, as determined by Eq. 10.

12. Summary

NIST and NMIJ have completed a bilateral comparison of their humidity standards. The quantity compared was the frost-point temperature produced by the generators of the two NMIs. A chilled-mirror hygrometer was used as the transfer standard. The nominal frost-point temperatures used for the comparison were –30 °C, –50 °C, –70 °C and –80 °C. The comparisons have determined the degree of equivalence between $[T_{FP}]_{NIST}$ and $[T_{FP}]_{NMIJ}$ at these points. For all frost-point temperatures over the range studied, the degree of equivalence is within 0.06 °C. All values for the degree of equivalence are within their expanded k = 2 uncertainties. The results allow a calculation of the degree of equivalence between $[T_{FP}]_{NIST}$ and $[T_{FP}]_{KCRV}$ at –30 °C and –50 °C. All values for this degree of equivalence are within 0.05 °C and within the expanded k = 2 uncertainties.

13. References

[1] S. Bell et al., Final report to the CCT on key comparison CCT-K6 – Comparison of local realisations of dew-point temperature scales in the range –50 °C to +20 °C, *Metrologia*, **52,** 03005 (2015).

[2] A. Saul and W. Wagner, "International Equations for the Saturation Properties of Ordinary Water Substance", *J. Phys. Chem. Ref. Data* **16,** 893−901 (1987).

[3] W. Wagner and A. Pruss, "International Equations for the Saturation Properties of Ordinary Water Substance--Revised According to the International Temperature Scale of 1990", *J. Phys. Chem. Ref. Data* **22**, 783−787 (1993).

[4] R.W. Hyland and A. Wexler, "Formulations for the Thermodynamic Properties of Dry Air from 173.15 K to 473.15 K, and of Saturated Moist Air from 173.15 K to 372.15 K, at Pressures to 5 MPa.", *ASHRAE Trans.* **89-IIa**, 520−535 (1983).

[5] International Association for the Properties of Water and Steam, Revised Release on the Pressure along the Melting and Sublimation Curves of Ordinary Water Substance (2011), available at www.iapws.org.

[6] Wagner, W., Riethmann, T., Feistel, R., and Harvey, A. H., "New Equations for the Sublimation Pressure and Melting Pressure of H_2O Ice Ih", *J. Phys. Chem. Ref. Data* **40,** 043103 (2011).

[7] C.W. Meyer et al., "Calibration of Hygrometers with the Hybrid Humidity Generator", NIST Special Publication 250-83 (2008).

[8] N. Ochi, C. Takahashi, H. Kitano, "Uncertainty of a New NMIJ Frost-Point Generator", Papers from the 4th International Symposium on Humidity and Moisture, 61-67 (2002).

[9] H. Abe, H. Kitano, N. Matsumoto, C. Takahashi, "Uncertainty analysis for trace-moisture standard realized using magnetic suspension balance/diffusion-tube humidity generator at NMIJ", *Metrologia* **52,** 731–740 (2015).

[10] D. Sonntag, "Important new values of the physical constants of 1986 vapor pressure formulations based on the ITS-90, and psychrometer formulae", Z. Meteorol. **70,** (1990) 340–344.

[11] L. Greenspan, "Functional Equations for the Enhancement Factors for CO_2 -Free Moist Air", J. Res. Natl. Bur. Stand., **80A,** 41-44 (1976).

[12] H. Abe, "Novel Flow Measurement/Control System in Magnetic Suspension Balance/Diffusion-Tube Humidity Generator", Int. J. Thermophys. **33,** 1500-1510 (2012).

[13] Thunder Scientific Model 2500 Data Sheet, http://www.thunderscientific.com/humidity_equipment/model_2500.html.

[14] Thunder Scientific Model 2500 Owners Manual, http://www.thunderscientific.com/tech_info/manuals/2500-System-Manual-Ed13.pdf.

[15] K.D. Hill, NRC Humidity Calibration Facility, Report Prepared in Support of SIM.T-K6.1: Realizations of local scales of dew/frost-point temperature of humid air, April 2015 (attached)